

# PARAMETERS DESIGN OF AUTONOMOUS DOCKING MODULE AND THE CHOICE OF SUITABLE TARGET AND PRIMARY PAYLOAD FOR ADR

O. G. Lagno<sup>(1)</sup>, T. I. Lipatnikova<sup>(1)</sup>, Yu. N. Makarov<sup>(2)</sup>, T. V. Mironova<sup>(1)</sup>, V. I. Trushlyakov<sup>(3)</sup>,  
Ya. T. Shatrov<sup>(4)</sup>, V. V. Yudintsev<sup>(1)</sup>

<sup>(1)</sup>JSC SRC Progress, 18, Zemetsa str., Samara, Russia

<sup>(2)</sup>Roscosmos, 42, Schepkina str., Moscow, Russia

<sup>(3)</sup>Omsk State Technical University, 11, Mira ave, Omsk, Russia

<sup>(4)</sup>TsNIIMash, 4, Pionerskaya str., Moscow, Russia

## ABSTRACT

The article deals with a problem of active removal of spent rocket bodies from Low Earth Orbits (LEO) using remaining fuel of upper stages after fulfillment of their primary mission of payload injection into orbit. It presents two possible ways of gripping and removal of a chosen piece of space debris. The first one uses the upper stage itself to grip the target object and remove it from orbit and the other uses an autonomous docking module, which is to be installed on the upper stage and separated from it tether-connected in the neighborhood of a target object. The article analyzes main mission phases such as approaching a target object of space debris, docking using a mechanism of probe-cone type, stabilization of the stack and its removal from orbit. The article gives comparison of these two methods.

## 1 INTRODUCTION

At present in near-earth orbits, there are over 1,600 rocket bodies with a total mass of about 2,700 tons including over 800 bodies with a total mass of over 1,198 tons in Low Earth orbits (LEO) [1]. Space debris objects are concentrated at altitudes of 850-1,500 km and in the geostationary orbit region [2], where they can stay for hundreds of years. To lower the risk of avalanche-like growth in the debris population, it is necessary to actively remove large-size objects [4,5] from orbits in the most active use [3].

The rocket bodies in LEO can be classified according to their mass and size. The performed analysis revealed that the most of rocket bodies in LEO (more than 400 objects) have a mass of 1,000-1,600 kg [1]. Since the rocket bodies have a simple symmetric form, they are ideal candidates for first experimental (demonstration) missions of active de-orbiting.

There are a lot of papers proposing different methods of active removal of space debris objects [6,7,8]. Nets [9,10,11], harpoons [12] can be used to capture such objects. A promising solution is to use a main engine nozzle of a rocket body for docking [13,14], which can be considered as a docking port for a probe-cone type

docking device [15,16,17,18].

Active debris removal (ADR) can be done using space tugs, specially developed to fulfill such tasks. This would obviously require great financial efforts associated with space tug development, building, launching and operation. To reduce costs, reusable space tugs can be used [19,20] or, which seems more reasonable, upper stages [21] can be used as *space tugs* after fulfillment of their primary mission – payload injection into orbit.

To fulfill the task of gripping a piece of space debris (target object), the upper stage should have a capability to identify the target object, determine parameters of its center-of-mass and attitude motion, to approach the target object and capture it. Such tasks are not customary for upper stages so it is necessary to install additional equipment on them. The present article, considers two possible ways to fulfill the task of space debris removal.

*Case A.* A nonseparable service platform is installed onto the upper stage that hosts necessary auxiliary supporting equipment and a device to grip a target object (Fig. 1).

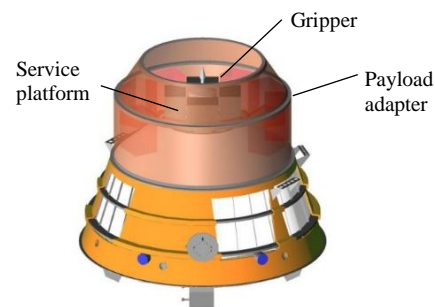


Figure 1. Case A

*Case B.* In this case, it is proposed to separate functions of tugging and gripping. An autonomous docking module (ADM) is installed onto the upper stage and connected to it with a tether (Fig. 2).

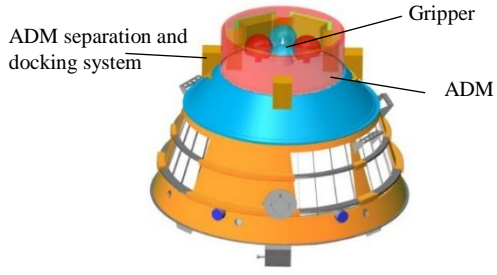


Figure 2. Case B

All necessary equipment to grip a space debris object or dock with it is installed on the ADM, which separates from the upper stage after arrival in the neighborhood of the target object [13]. The ADM will maneuver in the neighborhood of the target object, grip it and return to the upper stage for the follow-up removal. The upper stage should have equipment to separate the ADM, to control the tether, and to dock with the ADM, which gripped a piece of space debris.

The article comprises an introduction, two sections and conclusions. For the above-mentioned two cases, the second section gives main performance characteristics of the upper stage to be used as a space tug for active debris removal. The third section describes mathematic models of each mission phase and gives preliminary analysis of main parameters of the upper stage based on the developed models and compares the cases in consideration.

## 2 MAIN PERFORMANCE CHARACTERISTICS

Challenges of secondary mission of ADR are associated with limited capabilities of the upper stage to be used as a space tug. The upper stage that delivered its payload into orbit has a limited propellant supply to use for approaching a space debris object, gripping and removing it to a graveyard orbit. Propellant mass necessary for deorbiting maneuver depends on the altitude of the orbit where the space debris object is and on the mass of the stack of the upper stage and the target object (Fig. 3).

The upper stage's attitude control system limits disturbing moments that can influence upon the upper stage in the process of active removal of a space debris object. The disturbing moment can result from displacement of the center of mass of the tugged space debris object with respect to the longitudinal axis of the upper stage, caused by the specifics of the docking process of the space debris object with the upper stage.

For example, stability and controllability of the upper stage at different flight phases with its thruster in operation is determined by the following relation:

$$\text{atan}(Y_{max}/X_{min}) \leq 0.05236, \quad (1)$$

where  $Y_{max}$  is the maximum distance along Y-axis to the center of mass of the upper stage,  $X_{min}$  is the maximum distance along X-axis to the center of mass of the upper stage.

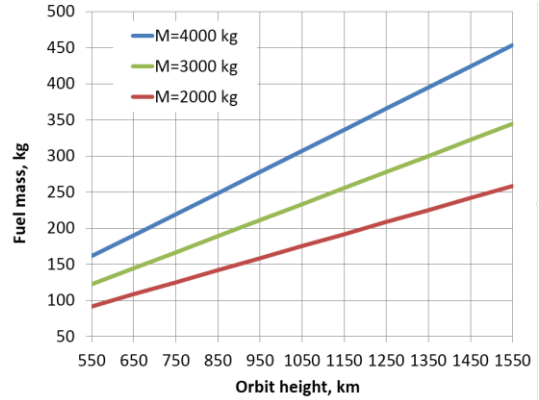


Figure 3. Fuel Mass Necessary for Deorbiting Maneuver from circular orbit

Besides, before tugging, the upper stage control system should stabilize the stack, that is to reduce its possible angular velocity caused by initial motion about the center of mass of a target object before docking and disturbances of its angular motion after docking.

Preliminary analysis showed that propellant consumption will not exceed 900 kg in the proposed demonstration experiment with an upper stage. Propellant consumption for each phase of the mission is specified in Tab. 1.

Table 1. Phase-by-Phase propellant consumption

Phase	Propellant mass, kg
Payload orbit injection	300...400
Far range rendezvous phase	100...200
Short range rendezvous phase, docking, stack stabilization	10...50
Deorbiting maneuver	100...450

The targets should be chosen subject to assessments of the upper stage propellant consumption necessary to approach the target object after payload injection, grip it and stabilize the stack and to remove it from orbit. To choose a target object it is necessary to analyze the center-of-mass and attitude motion of a target object. Such preliminary analysis can be made using ground observation facilities [22].

In view of the above-mentioned challenges of the demonstration experiment, the two proposed ways of using an upper stage for active removal of space debris are analyzed below.

## 2.1 CASE A (USING SERVICE PLATFORM)

In this case, a service platform is installed onto an upper stage. It comprises a power supply system, thermal control system, system of movable ballast masses, gripper, and onboard control complex with a control, navigation and orientation system, radar, telemetry system. Mass data of the system for case A are given in Tab. 2.

The system of movable ballast masses will allow partially compensate possible displacement of the center of mass of the stack with respect to the line of action of the upper stage's main thruster. Movable ballast with mass of 200 kg allows to fulfill ratio (1) even if the distance between the longitudinal axis of the upper stage (space tug) and the longitudinal axis of the debris is 0.3 m. The system of four movable masses allow to compensate center of mass position of the stack along all transverse axes.

Table 2. Mass of Components of the upper stage (Case A)

Component	Mass, kg
<b>Upper stage with propellant</b>	<b>1,240</b>
<b>Service platform</b>	<b>1500</b>
Gripper	50
Onboard equipment, battery	330
Movable ballast masses	900
Structure	220
Payload adapter	100
<b>Total mass</b>	<b>2,840</b>

Demonstration experiment solves the following tasks (Fig. 4):

- 1) Performing the maneuver of long-distance approach to the neighborhood of the chosen target object;
- 2) Short-distance aiming using a radar and video cameras;
- 3) Alignment of the upper stage's longitudinal axis and line of sight with zeroing of relative velocity of two objects;
- 4) Docking of the upper stage with the target object using the docking device within radio visibility of ground control stations;
- 5) Zeroing of angular momenta of the upper stage/target object stack by the upper stage's propulsion system;
- 6) Determination of mass and center-of-mass position of the stack using calibration pulses;
- 7) Correction of center-of-mass position of the stack using movable ballast weight (if necessary);
- 8) Performing the stack deorbiting maneuver using the

upper stage's propulsion system.

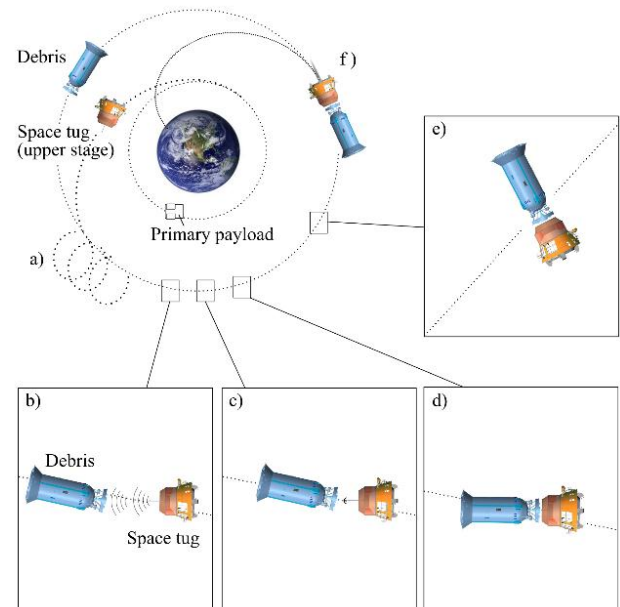


Figure 4. Phases of ADR Using an Upper Stage (space tug) with a service platform (case A)

Based on the data obtained from both ground facilities and onboard cameras during the first three phases, a control program is generated to approach the chosen target and grip it. The phases of long- and short-distance aiming are executed using control algorithms well-known and described in literature [23].

Taking into consideration possible angular motion of a target object, docking may be performed at high relative velocities as compared to conventional spacecraft docking where the relative docking velocity does not exceed 0.5 m/s.

After docking and forming a rigid connection between the upper stage and the target object, angular moment of this stack is zeroed using the upper stage's propulsion unit. At that or after that, the stack's moments of inertia, mass and center-of-mass position are assessed using calibration pulses. By the assessment results, the position of the stack's center of mass can be corrected using movable ballast weight.

The maneuver of stack deorbiting or its transfer into graveyard orbit is performed using the upper stage's propulsion system.

Masses of the upper stage and propellant for each phase of the mission are given in Tab. 3. The power capabilities of the upper stage allow to deorbit 4200 kg (debris mass about 1600 kg) from a 1000 km circular orbit.

Table 3. Upper stage mass report (Case A)

Flight event	Mass, kg	
	Upper Stage mass	Propellant mass
After the separation from the carrier	5500-7500	900
After the separation of the main payload	2740	400
After the long-range guidance phase	2640	300
After the docking with the target	4200	300

## 2.2 CASE B (USING AUTONOMOUS DOCKING MODULE)

Let's consider a case of active debris removal using the ADM, which is an autonomous space vehicle with a propulsion unit, control system and gripper.

After payload separation, the upper stage changes its orbit to approach the chosen target with minimum propellant consumption and then separate the ADM. At this phase, parameters of the target's orbital motion that were earlier determined by ground observation data are verified. Use of the ADM module makes unnecessary the zeroing of relative velocity between the upper stage and the target. This task is fulfilled by the ADM.

At the next phase of short-distance aiming, the autonomous docking module separates from the upper stage, and compensates the errors of the first phase using its own propulsion system, then determines parameters and generates a model of angular motion of the space debris object [22,24,25,26], corrects its own motion to create the most favorable conditions for docking. The upper stage adjusts its angular position to avoid tangling of the tether (Fig. 5a).

At the third phase, docking, the autonomous docking module rigidly connects to the space debris object (Fig. 5b). After docking, the stack is assembled. At this phase using its tether system, the upper stage brings the stack of the ADM and space debris object to its docking unit to dock with the ADM and form a rigid connection. To reduce the stack's angular velocity caused by shortening of the tether, engines of the upper stage and ADM are used (Fig. 5c).

After the phase of upper stage docking with the ADM stack (Fig. 5d), the stack's moments of inertia, mass and center-of-mass-position [27] are assessed, a control program is generated to deorbit the stack or to transfer it to a graveyard orbit (Fig. 5e).

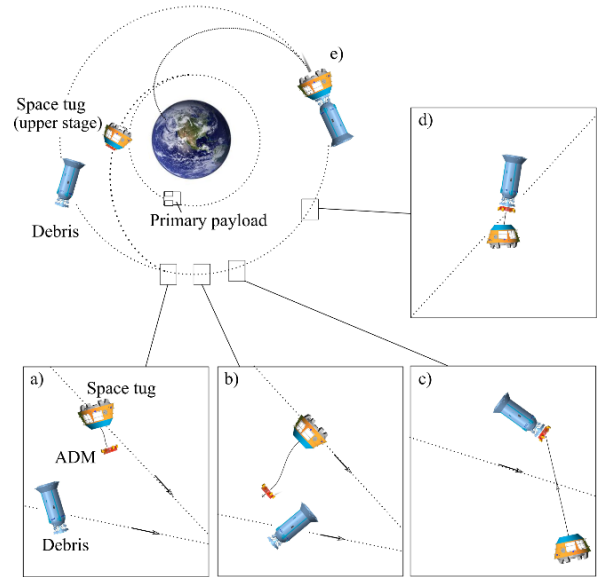


Figure 5. Phases of Space Debris Removal Using an ADM

To reduce propellant consumption for docking of the ADM with the upper stage after gripping the target, a tether is used, which is often considered as a component of the active debris removal system [28,29,30]. The length of the tether is determined by relative motion of the upper stage, target and ADM before and after ADM docking with the target.

Mass data of the system for case B are given in Tab. 4.

Table 4. Mass of Components of the upper stage (Case B)

Component	Mass
<b>Upper stage with nonseparable compartment:</b>	<b>1,580</b>
Fuelled upper stage	1,240
Structure with nonseparable compartment	340
<b>Autonomous docking module</b>	<b>260</b>
Gripper	50
Fuelled propulsion unit	75
Onboard equipment	85
Structure	50
Payload adapter	200
<b>Total mass</b>	<b>1,740</b>

Masses of the upper stage and propellant for each phase of the mission are given in Tab. 5.

Table 5. – Upper stage mass report (Case A)

Flight event	Mass, kg	
	Upper Stage mass	Propellant mass
After the separation from the carrier	5500-7500	900
After the separation of the main payload separation	2040	400
After the long-range guidance phase	1940	300
After the separation of the ADM	1680	300
After the docking with the ADM and space debris	3480	300

The power capabilities of the upper stage allow to deorbit the stack with mass of 3,500 kg from a circular orbit with height ~1150 km. In the Case B, the system of moving ballast masses is not installed.

### 3 MATHEMATICAL MODELS

To make a preliminary analysis of the above-mentioned cases of secondary mission of space debris removal, we developed a set of mathematical models of mission phases. Further we describe first approximation models – plane models of motion of the upper stage, ADM and debris object. To preliminary make quantitative assessments of the ADR phases, we use the following parameters of the upper stage, ADM and debris object that are given in Tab. 6.

Table 6. System Parameters

Parameter	Value
Mass of ADM, $m_1$ (See Tab. 3)	$2.6 \cdot 10^2$ kg
Mass of debris object, $m_2$	$2 \cdot 10^3$ kg
Mass of upper stage, $m_3$ (See Tab. 3)	$1.48 \cdot 10^3$ kg
Moment of inertia of ADM, $J_1$	$1 \cdot 10^2$ kg·m <sup>2</sup>
Moment of inertia of debris object, $J_2$	$1 \cdot 10^4$ kg·m <sup>2</sup>
Moment of inertia of upper stage, $J_3$	$1 \cdot 10^3$ kg·m <sup>2</sup>

#### 3.1 RELATIVE MOTION OF THE UPPER STAGE, ADM AND DEBRIS OBJECT

In case of using the upper stage for docking with a space debris object, the phase of approaching any space object by an upper stage is a known and well-tried procedure [23] and not considered herein.

In case of using an ADM, we assume a possibility to bring a space tug into the neighborhood of a space

debris object with a certain error caused by limited remaining fuel supply of the upper stage and limited capabilities of its control system. It seems possible to grip a target object if the upper stage moves in an elliptical orbit that “touches” the target object’s orbit. Below we consider a case of target object gripping where the upper stage moves in an elliptical orbit with a perigee radius  $r_p$  and apogee radius  $r_a$  after single-pulse maneuver, and the target object moves in a circular orbit with a radius  $r_a$  (Fig. 6).

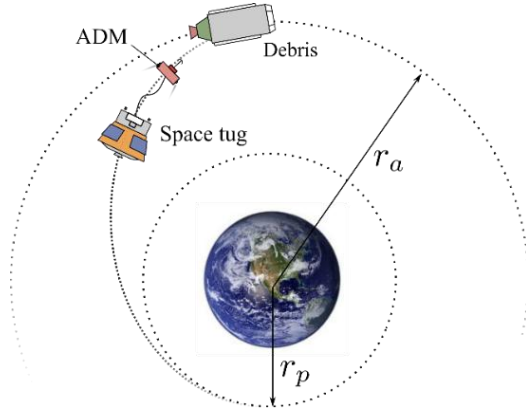


Figure 6. Orbits of the Upper Stage and the Space Debris Object

The difference of orbital velocities of the upper stage and the target object will be determined by the following equation:

$$\Delta V = \sqrt{\frac{\mu}{r_a}} (1 - \sqrt{1 - e}) \quad (2)$$

where  $e = (r_a - r_p)/(r_a + r_p)$  is the eccentricity of the upper stage orbit,  $\mu$  is the Earth gravitation parameter.

For example, in case of gripping a target object in a circular orbit with an altitude of 900 km from an elliptical orbit of 600×900 km, the difference of orbital velocities will be about 78 m/s. In the vicinity of a point of tangency of these two orbits, relative motion of the upper stage and the target object can be considered as rectilinear.

This difference of velocities can be compensated by the ADM after its separation from the upper stage. If the ADM moves with an acceleration  $a_1 = P_1/m_1$ , where  $m_1$  is the mass of the ADM,  $P_1$  is the thrust of the ADM’s engine, the time necessary to increase the velocity of the ADM relative to the upper stage up to the value  $\Delta V$  can be approximated by the following expression

$$\Delta t_1 \approx \frac{m_1}{P_1} \sqrt{\frac{\mu}{r_a}} (1 - \sqrt{1 - e}) \quad (3)$$

The length of the tether connecting the ADM and upper

stage will lengthen up to

$$\Delta L_I \approx \frac{P}{2 m_1} \Delta t_I^2 \quad (4)$$

At that, the initial distance between the target object and the upper stage at the moment of ADM separation should be no less than (Fig. 7)

$$s_0 \approx \Delta V t_I - \frac{P_1}{2 m_1} t_I^2 \quad (5)$$

For the above-mentioned orbital parameters of the target object and the upper stage, the ADM's mass  $m_1 = 200$  kg, the engine thrust  $P_1 = 500$  N, we obtain  $\Delta t_I \approx 30$  s, the tether length  $\Delta L_I \approx 1.2$  km and initial distance  $s_0 \approx 1.2$  km. To perform this maneuver, the ADM will consume about 7 kg of fuel (at the ADM engine's specific impulse of 250 s).

It should be noted that fuel consumption for changing the upper stage's orbit will be higher in the first case. Transfer of the upper stage into the target object's orbit will require a double-pulse maneuver. For example, for the above-mentioned orbital parameters, the upper stage's increment velocity after the first pulse will be about 79 m/s, after the second pulse it will be 78 m/s and that will require about 130 kg of fuel (at the ADM engine's specific impulse of 250 s). In the example under consideration, use of the ADM will allow reducing fuel consumption by about 50%.

After ADM docking with a target object, this stack continue moving relative to the upper stage at a velocity  $\Delta V = V_{12} - V_3 \approx V_2 - V_3$ . To reduce the relative velocity, it is necessary to control the tether length. Let us assume that the tether length changes uniformly decelerating with a negative acceleration  $a = \Delta V / t_k$ , where  $t_k$  is the time of tether length control up to reaching a zero relative velocity. According to the chosen law, the maximum tether length will be determined by the equation

$$L_{II} = L_I + \Delta V \frac{t_k}{2} \quad (6)$$

The uniformly decelerated motion of the ADM and target object relative to the upper stage is provided by the tether tension, which is equal to the following:

$$T = \frac{\Delta V}{t_k} m_{12} \quad (7)$$

The tension value should not exceed a certain maximum value  $T_{max}$ , which is determined by strength of the structural elements, tether control device and tether. Eq. 6 implies the following time limitation for tether system deceleration:

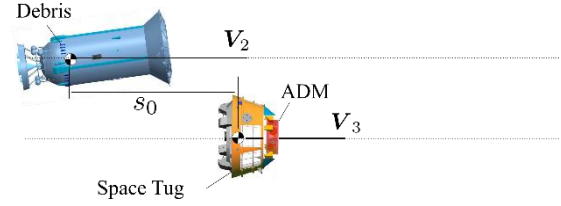
$$t_k > \frac{\Delta V}{T_{max}} m_{12} \quad (8)$$

And the following limitation of the tether length:

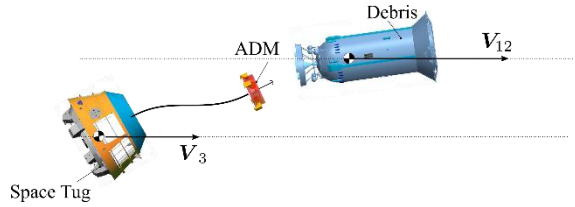
$$L_{II} > \frac{P}{2 m_1} \Delta t_I^2 + \frac{\Delta V^2}{2 T_{max}} m_{12} \quad (9)$$

For the above-mentioned orbital parameters of the target object and the upper stage, ADM parameters and tether material of Spectra 2000 type [31] with a cross-section  $S = 10$  mm<sup>2</sup>, the maximum tether tension should not exceed 30 kN. The time of decrease in relative velocity between the target object and upper stage down to zero is no less than 6 seconds.

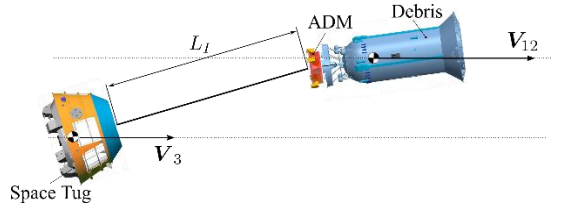
a) Separation of the ADM from the upper stage



b) Shortening of distance between the ADM and the target object



c) Target object gripping (ADM docking with the target object)



d)

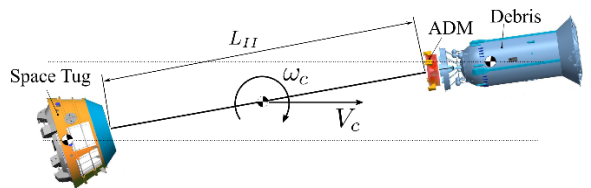


Figure 7. Phases of Relative Motion of the ADM and Target Object during Formation of a Tethered System

### 3.2 MODEL OF DOCKING

This section is devoted to the model of docking an active remover, which can be an upper stage or autonomous docking module, with a space debris object of an upper-stage type. A well-known probe-cone mechanism is used for docking. The nozzle of a rocket body's main engine is used as a docking port. The probe is gimbal mounted to the active remover. To

compensate impacts when the probe contacts the nozzle surface, the hinge is equipped with damping devices.

When developing a mathematical model, it is supposed that ADM docking with a space debris object is a rapid process, which allows neglecting influence of the gravitational field and other forces upon bodies under consideration.

The system layout is shown in Fig.8.

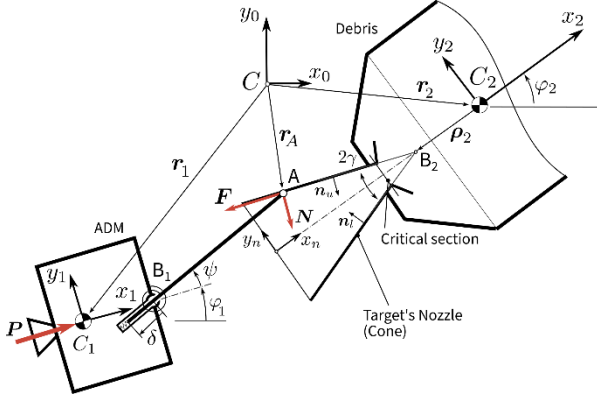


Figure 8. Model of Probe-Cone Docking

We consider plane motion of three bodies – a space debris object, docking module (ADM or upper stage), and a docking probe. The probe of the docking device is hinged to the docking module (hinge  $B_1$ ), at that it is assumed that the probe rotates with regard to the active remover (generalized coordinate  $\psi$ ) and advances along its longitudinal axis (generalized coordinate  $\delta$ ). Damping hinge force and moment reduce impact action on the active remover when the probe contacts the nozzle surface:

$$Q_\psi = -c_\psi \dot{\psi} - k_\psi \psi \quad (10)$$

$$Q_\delta = -c_\delta \dot{\delta} - k_\delta \delta \quad (11)$$

where  $c_\psi$ ,  $k_\psi$  are the torsional stiffness and damping coefficient,  $c_\delta$ ,  $k_\delta$  are the stiffness and damping coefficient of the translational motion of the probe relative to the docking module.

The target object's nozzle is approximated by the conical surface, which – in this two-dimensional case under consideration – is represented by two segments inclined at the angle  $\gamma$  to the target object's longitudinal axis and crossing at the point  $B_2$  of the longitudinal axis.

Equations of motion for the docking module (5 motion equations) and the target object (3 motion equations) that are integrated independently with control of distance from the nozzle surface to the point A. In case one of two distances becomes equal to zero, the integration process stops and the bodies' velocity discontinuities are determined according to the theory of perfectly inelastic collision. After that, equations integration is continued together with a constraint

equation, describing motion of the point A along the nozzle surface.

### 3.2.1 Statistical Modelling

To study the docking process the Monte-Carlo method is used. The docking is considered successful when the tip of the docking device's probe (point A) crosses the critical section of the orbital stage's nozzle.

We studied what effect the following parameters had upon success of docking at the moment when the probe's point A crossed the nozzle exit section (Fig. 9): projections of docking module velocity to its own axes  $V_{1x,0}^{(1)}$ ,  $V_{1y,0}^{(1)}$ ; initial angular position of the docking module  $\varphi_{1,0}$ ; displacement of the probe's point A from the orbital stage's longitudinal axis  $y_0$ ; initial angular velocity of the orbital stage.

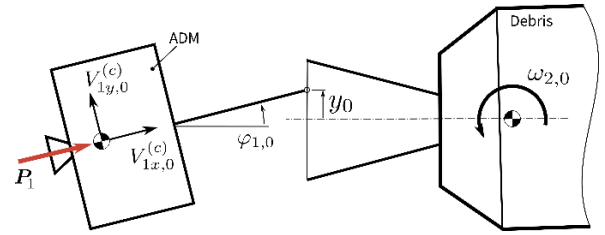


Figure 9. Initial Docking Conditions

Docking device parameters are given in Tab. 7.

Table 7. Parameters of the Docking Device and the Nozzle

Parameter	Value
Stiffness, $c_\psi$	$10^2 \text{ N} \cdot \text{m}/\text{deg}$
Damping coefficient, $k_\psi$	$10 \text{ N} \cdot \text{m} \cdot \text{s}/\text{deg}$
Stiffness, $c_\delta$	$10^5 \text{ N}/\text{m}$
Damping coefficient, $k_\delta$	$10^2 \text{ N} \cdot \text{s}/\text{m}$
Probe length	1.5 m
Probe mass	5 kg
Nozzle diameter	1.2 m

We considered two cases of docking. In the first case, the active remover is an ADM and in the second case it is an upper stage. 10,000 calculations were performed using the Monte-Carlo method where initial conditions were considered as random variables uniformly distributed in specified ranges given in Tab. 8.

We considered four estimated cases: upper stage docking under initial conditions specified in Tab. 5 and zero thrust  $P_1$ ; upper stage docking under initial conditions specified in the table and thrust  $P_1=3,000 \text{ N}$ ; ADM docking under initial conditions specified in the table and zero thrust  $P_1$ ; ADM docking under initial conditions specified in the table and thrust  $P_1 = 500 \text{ N}$ .

Fig. 10 shows dependences of successful docking probability on projections of initial velocity of the docking module (ADM or upper stage) to its longitudinal axis.

Table 8. Initial Docking Conditions

Parameter	Value
$V_{1x,0}^{(1)}$	0.5 to 10 m/s
$V_{1y,0}^{(1)}$	minus 0.5 to 0.5
$\varphi_{1,0}$	minus 45 to 45 degrees
$y_0$	minus 0.55 to 0.55 m
$\omega_{2,0}$	minus 15 to 15 °/s

The probability of successful ADM docking without engine activation is lower than probability of successful upper stage docking in the whole range of velocities, which is explained by lower mass and therefore lower kinetic energy of the ADM at the moment of probe crossing of the nozzle exit section. The diagrams show obvious increase in probability of successful docking with increase of initial approaching velocity of the active remover and orbital stage. The ADM's engine thrust has marked influence on the probability of successful docking, if the ADM moves with an acceleration of  $0.25 \text{ m/s}^2$ , the probability of successful docking in the whole range of the ADM's longitudinal velocity of 0.5 to 10 m/s is more than 0.8

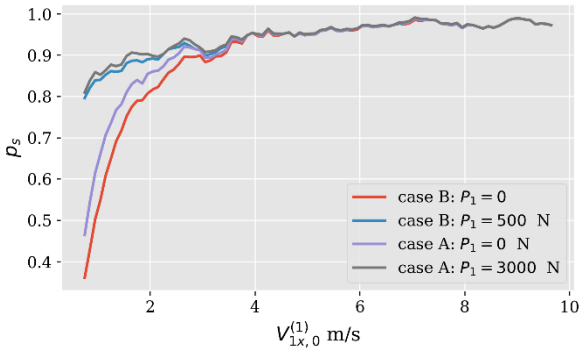


Figure 10. Dependence of the Successful Docking Probability on the Initial Velocity  $V_{1x,0}^{(1)}$

Fig. 11 shows distribution of points of successful (grey points) and failed (red points) docking depending on the active remover's initial velocity projected to its longitudinal axis and the initial position of the probe tip relative to the nozzle's longitudinal axis. An upper stage is considered as an active remover.

In the developed parameter region  $V_{1x,0}^{(1)}$ ,  $y_0$  we can single out a subset

$$V_{1x,0}^{(1)} \in [4; 10] \text{ m/c} \cap y_0 < 0.3 \text{ m} \quad (12)$$

where all points correspond successful docking of the upper stage.

It is obvious that with increase in initial velocity, loads acting on the docking mechanism increase too, and that should be taken into account in formation of the program to control the active remover at the phase of docking. For illustration purposes, Fig. 12 shows dependences of hinge moment in the probe hinge of the docking mechanism on the initial velocity  $V_{1x,0}^{(1)}$ .

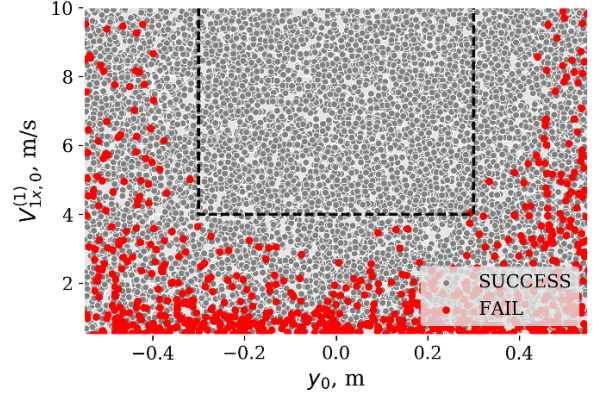


Figure 11. Distribution of Points of Successful Docking Depending on  $y_0$  and  $V_{1x,0}^{(1)}$

The large mass of the upper stage results in high hinge moments in the process of docking, at that, as mentioned above, use of ADM engine thrust for docking results in great increase in probability of successful docking but does not cause great increase in hinge moment.

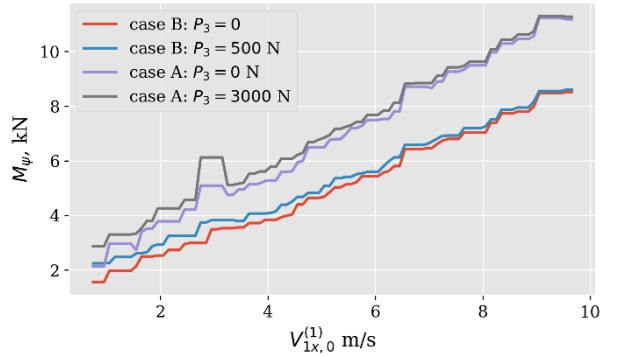


Figure 12. Dependence of the Probe Mount's Hinge Moment on the Approach Velocity of the docking module (Upper Stage or ADM)

### 3.3 TETHERED SYSTEM STABILIZATION

In case of use of an ADM for docking with a target object, it is supposed to use a tether to reduce fuel consumption for return of the ADM with a gripped target object and its docking with the upper stage (space tug). The tether connects the ADM and upper stage and its length and tension are controlled by the upper stage. The initial conditions of the tethered system motion after ADM docking with the space debris object are

determined by the relative motion velocities of the upper stage and space debris object. The angular velocity of this tethered system will be determined by the difference of projections of absolute velocities of the upper stage and space debris object to the line perpendicular to the tether. To dock the ADM with the upper stage after successful target object gripping, it is necessary to shorten the tether length. It will result in increase in angular velocity of the tethered system and consequently in increase in tension of the tether, which can cause its rupture.

Let us determine the propulsive force necessary to damp the tethered system angular velocity with simultaneous shortening of the tether length. Let us assume that the law of the tether length variation is linear

$$l(t) = l_0 - v_l t \quad (13)$$

where  $l(t)$  is the tether length at the time  $t$ ,  $v_l$  is the rate of the tether length change,  $l_0$  is the initial tether length. The theorem of variation of angular momentum of a system (Fig. 13) consisting of two material points with masses  $m_{12}$  and  $m_3$ , which are connected by a tether and rotating about the common center of mass, will have the appearance:

$$\frac{d}{dt}(J_c \omega_c) = -F_\psi \left[ (l + x_{12} + x_3) \frac{m_3}{m} - x_\psi \right] \quad (14)$$

where  $m_3$  is the mass of the upper stage,  $m$  is the mass of the system,  $J_c$  is the moment of inertia of the tethered system relative to its center of mass:

$$J_c = (l + x_{12} + x_3)^2 m^* \quad (15)$$

where  $m^* = m_{12} m_3 / (m_1 + m_3)$ . It is assumed that the ADM's engine propulsive force  $F_\psi$  is always perpendicular to the tether. Substituting Eqs. 13 and 15 into Eq. 14 and introducing a notation  $l^* = l_0 - v_l t + x_{12} + x_3$ , we obtain

$$\frac{F_\psi}{m_{12} l^*} \left( \frac{x_\psi m_{12}}{m_3} - l^* + x_\psi \right) = l^* \frac{d\omega_c}{dt} - 2v_l \omega_c \quad (16)$$

Integrating Eq. 16 with the initial condition  $\omega_c(0) = \omega_{c,0}$ , we shall obtain an equation for the force  $F_\psi$ , which is determined by a given time  $t_k$  of the tethered system's angular velocity variation to the value  $\omega_{c,0}$

$$F_\psi = \frac{2m_3 m_{12} [\omega_{c,0} \cdot (l_0^*)^2 - \omega_{c,k} \cdot (l_k^*)^2]}{m_3 (l_0^* + l_k^*) - 2(m_3 + m_{12}) x_\psi} \cdot \frac{1}{t_k} \quad (17)$$

where  $l_k^* = l_0 - v_l t_k + x_{12} + x_3$  is the final distance between the centers of mass of the upper stage and the ADM/target object stack.

It is obvious that the origin of  $F_\psi$  will not coincide with the center of mass of the ADM/target object stack ( $x_\psi \neq 0$ ), and that will cause turning of the stack relative to the tether (about the tether attachment point  $A_1$ ), deviation

of the line of action of the force from the line perpendicular to the tether, and violation of conditions, under which the solution of Eq. 17 is obtained. This is illustrated in Fig. 14. The figure shows variations of angles  $\varphi_3$  and  $\varphi_2$  during stabilization of the tethered system. Action of the force  $F_\psi$  on the stack of the ADM and target object causes increase in the angle  $\varphi_2$  – the angle of deviation of the ADM's longitudinal axis from the line of the tether – as the angular velocity of the tethered system decreases.

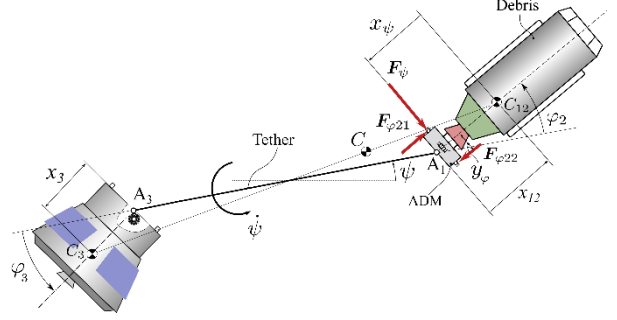


Figure 13. Tethered System

The results presented are obtained for the initial tether length  $l_0 = 200$  m, initial angular velocity  $\omega_{c,0} = 10^\circ/\text{s}$ ,  $t_k = 500$  s,  $l_k = 5$  m, center-of-mass positions of the upper stage and stack  $x_{12} = 4$  m,  $x_3 = 2$  m respectively, and the origin of the force  $x_\psi = 1.5$  m (Fig. 13). For the stated values, the force  $F_\psi$  is 311 N.

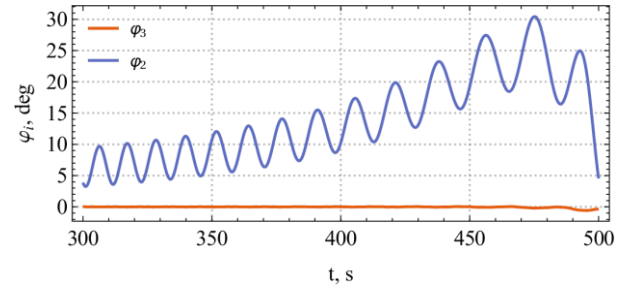


Figure 14. Deviations of the Upper Stage's Longitudinal Axis  $\varphi_3$  and the Stack's Longitudinal Axis  $\varphi_2$  from the Tether Line Caused by the force  $F_\psi$

Fig. 15 shows variation of the tethered system's angular velocity for this case. For comparison it also shows variation of angular velocity of the tethered system of two mass points of the same mass.

Deviation of the line of action of the force  $F_\psi$  from the line perpendicular to the tether results in failure of necessary reduction of the tethered system's angular velocity.

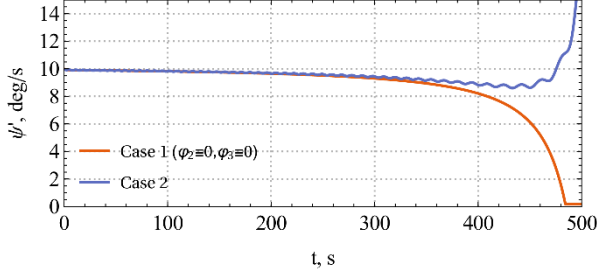


Figure 15. Angular Velocity Variation of the Tethered System of Mass Points and Solid Bodies

To reduce the turn of the target object relative to the tether attachment point  $A_1$ , it is necessary to involve the ADM's thrusters and the angular motion control system should control the angle and angular velocity of the ADM relative to the tether (the angle  $\varphi_2$  and angular velocity  $\dot{\varphi}_2$ ). Let us assume that a couple of forces ( $F_{\varphi 21}$ ,  $F_{\varphi 22}$ ) generated by the ADM's thrusters is applied to the ADM. The forces  $F_{\varphi 21}$ ,  $F_{\varphi 22}$  are directed along the target object's longitudinal axis. Assuming infinitesimality of the tethered system's angular acceleration under the action  $F_\psi$ , we can write down the condition of quasi-static equilibrium of the stack of the ADM and target object:

$$F_{\varphi 21} = -F_{\varphi 22} = \frac{F_\psi x_\psi - T x_{12} \sin \varphi_2}{2 y_\varphi} \quad (18)$$

For the small angle  $\varphi_2$ :

$$F_{\varphi 21} = -F_{\varphi 22} = \frac{F_\psi x_\psi - x_{12} \varphi_2}{2 y_\varphi} \quad (19)$$

After reduction of the tethered system's angular velocity to the value approximate to zero, contraction of the tethered system continues using thrusters of the ADM and upper stage to stabilize the bodies before docking. Fig. 16 shows variation of the tethered system's angular velocity when the force  $F_\psi$  successively acts on the tethered system in the interval 0 to 440 s and the control moment  $M_i = M_U U_i$ ,  $i = 2, 3$ , where

$$U_i = \begin{cases} -1, & \varphi_i > \varphi_i^{max} \text{ и } \dot{\varphi}_i > -\dot{\varphi}_i^{max} \\ 0, & |\varphi_i| < \varphi_i^{max} \text{ и } |\dot{\varphi}_i| < \dot{\varphi}_i^{max} \\ +1, & \varphi_i < -\varphi_i^{max} \text{ и } \dot{\varphi}_i < \dot{\varphi}_i^{max} \end{cases} \quad (20)$$

Fig. 17 shows variations of the ADM rotation angle  $\varphi_2$  and the upper stage rotation angle ( $\varphi_3$ ) relative to the tether. Maximum deviation is no more than 2 degrees.

So we showed that it is possible in principle to use a tether for ADM docking with the space tug. Use of the tether at this phase will allow simplifying the process of docking in case of gripping the target object without approaching it by the space tug.

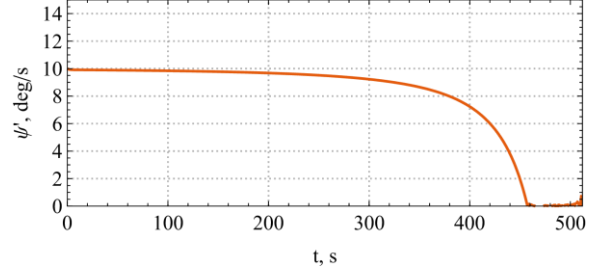


Figure 16. Variation of the Tethered System's Angular Velocity upon Action of Stabilizing Moments

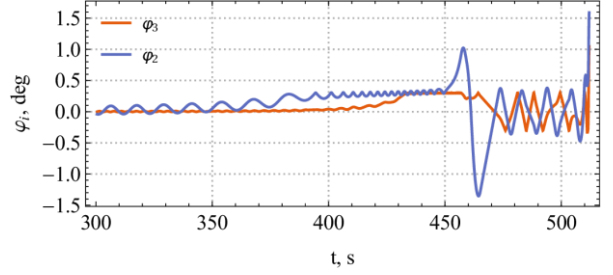


Figure 17. Deviations of Longitudinal Axes of the Upper Stage and the Stack upon Action of Stabilizing Moments

To reduce fuel consumption, it is necessary that the line of tether was oriented along the vector of relative velocity of the target object and the space tug. In this case it is possible to dramatically reduce fuel consumption for stabilization of the tethered system.

#### 4 CONCLUSIONS

1. The principal possibility of conducting the demonstration experiment on the ADR of large-sized space debris objects in the secondary mission is shown. We consider two cases of active removal of large-sized space debris objects as a secondary mission by an upper stage itself or using tethered autonomous docking module for target object gripping.

2. Comparative analysis of considered cases showed the advantages and disadvantages of each case. In case A a nonseparable service platform is installed onto the upper stage that hosts necessary auxiliary supporting equipment and a device to grip a target object. The control system of the orbital stage in case A should be able to perform navigation tasks with high accuracy to ensure the required conditions of docking taking into account limited maneuvering capabilities of the orbital stage. In case B the ADM can compensate errors of the upper stage control system, so high accuracy of the orbital stage control system is not required. This will require the development of the ADM with advanced control system and orbital maneuvering system. The smaller mass of the ADM in comparison with the orbital stage makes it more suitable for docking with tumbling rocket bodies.

3. The most difficult phase is gripping and docking of an ADM or upper stage with a space debris object. The probability of successful docking using a conventional mechanism of probe-cone type depends on the initial angular velocity of the target object when the probe crosses the nozzle exit section. At a velocity of more than 4 m/s, the probability of successful docking is more than 0.9. It is obvious that a higher velocity of docking causes higher loads acting on the docking device and probe mount when crossing the critical section of the nozzle.

4. When using an ADM, after its gripping of a target object, a tethered system is formed, kinematic parameters of which are determined by the relative motion of the upper stage and the target object. Preliminary analysis showed that stabilization of the tethered system with simultaneous shortening of the tether requires using the ADM's engines that should provide not only reduction of angular velocity of the tethered system but also the coincidence of the ADM's longitudinal axis and the line of the tether. To reduce fuel consumption for stabilization of the tethered system, it is necessary that at the moment of target object gripping – formation of a rigid connection between the ADM and the target object – the line of action of the tether coincides with the vector of relative velocity of the target object and the upper stage.

5. The capabilities of the upper stage and ADM make it possible to provide a demonstration flight experiment on the ADR of the second stage of Kosmos-3M rocket from circular orbits from 500 to 1500 km in height.

6. The choice of possible target for the demonstration experiment is determined by an amount of residual fuel of the upper stage after the separation of the main payload; operation time of the upper stage and its control system capabilities; ADM performance and attitude motion of the debris.

7. Further studies are supposed to specify the mathematic models presented herein in terms of analysis of the spatial motion of a space debris object and ADM in the process of docking using a mechanism of probe-cone type, analysis of the possibility of using other gripping methods such as with the help of a net, harpoon, lasso, manipulator.

## 5 ACKNOWLEDGMENTS

This study was partially supported by the Russian Science Foundation (Project No. 16-19-10158)

## 6 REFERENCES

1 Anselmo, L. and Pardini, C. (2016) 'Ranking upper stages in low Earth orbit for active removal'. *Acta Astronautica*, 122, pp. 19–27. [online] Available from:

<http://dx.doi.org/10.1016/j.actaastro.2016.01.019>

- 2 Liou, J. C. (2011) 'An active debris removal parametric study for LEO environment remediation'. *Advances in Space Research*, 47(11), pp. 1865–1876. [online] Available from: <http://dx.doi.org/10.1016/j.asr.2011.02.003>
- 3 Kessler, D. J. and Cour-Palais, B. G. (1978) 'Collision frequency of artificial satellites - The creation of a debris belt'. *Journal of Geophysical Research*, 83(A6), pp. 2637–2646. [online] Available from: <http://onlinelibrary.wiley.com/doi/10.1029/JA083iA06p02637/abstract>
- 4 Liou, J.-C. and Johnson, Nicholas L. (2009) 'A sensitivity study of the effectiveness of active debris removal in LEO'. *Acta Astronautica*, 64(2–3), pp. 236–243.
- 5 Ansdell, Megan (2010) 'Active Space Debris Removal: Needs, Implications, and Recommendations for Today's Geopolitical Environment'. *Journal of Public and International Affairs*, 21(1), p. 16.
- 6 Bonnal, Christophe, Ruault, Jean-Marc and Desjean, Marie-Christine (2013) 'Active debris removal: Recent progress and current trends'. *Acta Astronautica*, 85, pp. 51–60.
- 7 Aslanov, V. S. and Yudinsev, V. V. (2013) 'Dynamics of Large Debris Connected to Space Tug by a Tether'. *Journal of Guidance, Control, and Dynamics*, 36(6), pp. 1654–1660. [online] Available from: <http://arc.aiaa.org/doi/abs/10.2514/1.60976> (Accessed 1 July 2014)
- 8 Aslanov, V. S. and Yudinsev, V. V. (2015) 'Dynamics, analytical solutions and choice of parameters for towed space debris with flexible appendages'. *Advances in Space Research*, 55(2), pp. 660–667. [online] Available from: <http://linkinghub.elsevier.com/retrieve/pii/S0273117714006620>
- 9 Benvenuto, R and Lavagna, Mr (2013) 'Flexible Capture Devices for Medium To Large Debris Active Removal: Simulations Results To Drive Experiments'. *Robotics.Estec.Esa.Int.*, (1).
- 10 Botta, Eleonora M., Sharf, Inna, Misra, Arun K. and Teichmann, Marek (2016) 'On the simulation of tether-nets for space debris capture with Vortex Dynamics'. *Acta Astronautica*, 123, pp. 91–102.
- 11 Botta, Eleonora M., Sharf, Inna and Misra, Arun K. (2016) 'Contact Dynamics Modeling and Simulation of Tether Nets for Space-Debris Capture'. *Journal of Guidance, Control, and Dynamics*, 40(1), pp. 1–14.
- 12 Dudziak, Roger, Tuttle, Sean and Barraclough,

- Simon (2014) 'Harpoon technology development for the active removal of space debris'. *Advances in Space Research*.
- 13 Trushlyakov, V. I., Shatrov, Ya. T., Oleynikov, I. I., Makarov, Yu. N. and Yutkin, Ye. A. (2010) 'Sposob stykovki kosmicheskikh apparatov (The Method of Spacecraft Docking)'. In Russian. [online] Available from: <http://www.findpatent.ru/patent/252/2521082.html>
  - 14 Jones, Howard Martin, Malaviarachchi, Pat and Mackenzie, Andrew Charles (2005) 'Spacecraft Docking Mechanism'. , 1(12).
  - 15 Moody, Clark K, Probe, Austin B, Masher, Abhay, Woodbury, Timothy, et al. (2016) 'Laboratory Experiments for Orbital Debris Removal', in *AAS Guidance, Navigation, and Control Conference*, Breckenridge, CO, pp. 1–12.
  - 16 Yoshida, Kazuya, Nakanishi, Hiroki, Ueno, Hiroshi, Inaba, Noriyasu, et al. (2004) 'Dynamics, control and impedance matching for robotic capture of a non-cooperative satellite'. *Advanced Robotics*, 18(March), pp. 175–198.
  - 17 Han, Wei, Huang, Yiyong and Chen, Xiaoqian (2014) 'Research of impact dynamic modeling of flexible probe-cone docking mechanism based on Kane method'. *Archive of Applied Mechanics*, 85(2), pp. 205–221. [online] Available from: <http://dx.doi.org/10.1016/j.asr.2011.12.030>
  - 18 Yaskevich, Andrey (2014) 'Real Time Math Simulation of Contact Interaction during Spacecraft Docking and Berthing'. *Journal of Mechanics Engineering and Automation*, 4, pp. 1–15.
  - 19 Barbee, Brent W., Alfano, Salvatore, Pi??on, Elfego, Gold, Kenn and Gaylor, David (2012) 'Design of spacecraft missions to remove multiple orbital debris objects', in *Advances in the Astronautical Sciences*, IEEE, pp. 93–110.
  - 20 Savioli, L, Francesconi, A, Maggi, F, Olivieri, L, et al. (2013) 'Space Debris Removal Using Multi-Mission Modular Spacecraft', in *6th European Conference on Space Debris*, Darmstadt, Germany, pp. 22–25.
  - 21 Anshakov, G. P., Grigoryev, S. K., Manturov, A. I., Panov, N. A. and Poplevin, A. S. (2013) 'Evaluation of spacecraft injection accuracy by Volga upper stage', in *20th Saint Petersburg International Conference on Integrated Navigation Systems, ICINS 2013 - Proceedings*, pp. 376–382. [online] Available from: <http://www.scopus.com/inward/record.url?eid=2-s2.0-84894208982&partnerID=tZOTx3y1>
  - 22 Lichter, M.D. and Dubowsky, S. (2004) 'State, shape, and parameter estimation of space objects from range images'. *IEEE International Conference on Robotics and Automation, 2004. Proceedings. ICRA '04. 2004*, 3(April), pp. 2974–2979.
  - 23 Fehse, W. (2003) 'Automated Rendezvous and Docking of Spacecraft'. *System*.
  - 24 Fang, Jia Qi and Huang, Thomas S. (1984) 'Some Experiments on Estimating the 3-D Motion Parameters of a Rigid Body from Two Consecutive Image Frames'. *IEEE Transactions on Pattern Analysis and Machine Intelligence*, PAMI-6(5), pp. 545–554.
  - 25 Hillenbrand, Ulrich and Lampariello, Roberto (2005) 'Motion and parameter estimation of a free-floating space object from range data for motion prediction'. *European Space Agency, (Special Publication) ESA SP*, (603), pp. 461–470.
  - 26 Masutani, Yasuhiro, Iwatsu, Takeshi and Miyazaki, Fumio (1994) 'Motion Estimation of Unknown Rigid Body under No External Forces and Moments'. *International Conference on Robotics and Automation*, pp. 1066–1072.
  - 27 Bergmann, E. V., Walker, B. K. and Levy, D. R. (1987) 'Mass Property Estimation for Control of Asymmetrical Satellites'. *Journal of Guidance, Control, and Dynamics*, 10(5), pp. 483–491.
  - 28 Cartmell, M. P. and McKenzie, D. J. (2008) 'A review of space tether research'. *Progress in Aerospace Sciences*, 44(1), pp. 1–21.
  - 29 Qi, Rui, Misra, Arun K. and Zuo, Zongyu (2016) 'Active Debris Removal Using Double-Tethered Space-Tug System'. *Journal of Guidance, Control, and Dynamics*, pp. 1–9. [online] Available from: <http://arc.aiaa.org/doi/10.2514/1.G000699>
  - 30 Mantellato, R., Olivieri, L. and Lorenzini, E.C. (2016) 'Study of dynamical stability of tethered systems during space tug maneuvers'. *Acta Astronautica*, (July), pp. 1–10.
  - 31 Pearson, Jerome, Levin, Eugene, Oldson, John and Wykes, Harry (2005) *Lunar Space Elevators for Cislunar Space Development. Phase I Final Technical Report*, Mount Pleasant.